SOME SPECIFIC FEATURES OF THE PULSE LASER RADIATION ABSORPTION IN THE ATMOSPHERE

Yu.V. Kistenev and V.A. Filimonova

Tomsk State University
Received November 3, 1995

Some peculiarities of attenuation of laser pulses during their propagation in a resonantly absorbing medium over slant and vertical atmospheric paths are analyzed in the paper. A plane-layered atmospheric model is considered. Calculations take into account the altitude variations of shape, width, and center of an absorption line and the concentration of an absorbing gas. The transmission of the medium is examined as a function of the radiation propagation direction. The influence of the absorption line center shift due to air pressure on this parameter is also considered. The estimates have been obtained for laser generation lines in the spectral region of the atmospheric water vapor absorption.

The choice of the atmospheric water vapor as a resonantly absorbing component is caused by the fact that its dynamics in the atmosphere determines the conditions of weather formation in many respects, so the water vapor is a traditional object of laser sounding. Besides, water vapor has a developed spectrum with large absorption bands in the visible and IR ranges.

In this paper, we present estimates of the atmospheric transmission during pulse laser radiation propagation along slant and vertical paths for laser generation lines in the spectral region of the atmospheric water vapor absorption. Ruby, YAG, carbon dioxide, and atomic iodine lasers are investigated. The estimates are obtained under conditions of linear interaction of the optical radiation with the medium.

Taking into account various effects of interaction nonstationarity including nonstationary refraction[2,3] (i.e., change of the direction of beam propagation in an inhomogeneous medium when its refractive index varies in time because of interaction nonstationarity) and the absorption line center shift due to air pressure are new aspects in the formulation of the given problem as compared with the standard transmission characteristics.[1] The influence of the line center shift on the atmospheric transmission was estimated in Ref. 4 for monochromatic radiation and in Ref. 5 for pulse radiation with the use of the Fourier transform.

In Ref. 2 it was first demonstrated that the characteristics of the transmitted radiation may depend on the direction of propagation when short optical pulses are propagated along slant atmospheric paths under conditions of resonant absorption of the medium. This is caused by temporal variations of the refraction angle of a radiation beam due to nonstationarity of its interaction with the medium. As a consequence, phase run-on of spectral components of the radiation and, in the end, the pulse shape will depend on the inhomogeneity structure of the medium. In particular, the transmitted pulse shape changes for the reverse propagation direction.

A straightforward analysis of this problem in a spatiotemporal domain[3] has demonstrated that this approach is more correct as compared with the method of the Fourier transform because additional (in comparison with a homogeneous medium) phase pulse modulation arising due to nonstationary refraction cannot be taken into account in a frequency domain. A consideration of pulse modulation, as demonstrated in Ref. 3, resulted in the dependence of the transmission of the medium on the direction of radiation propagation. Below, we use the approach developed in Ref. 3.

Since most of the atmospheric water vapor is concentrated in the tropospheric layer, the thickness of the atmospheric layer was chosen to be equal to 10 km in our calculations. It is obvious that for such altitudes the inhomogeneous atmosphere can be modeled as a plane-layered inhomogeneous medium whose parameters correspond to standard statistical models.[6] The changes of the shape, width, and frequency shift of the absorption line as well as of the concentration of the resonant component with altitude were taken into account in the calculations. The resonant component of the refractive index of the medium also underwent similar changes in accordance with the Kramers-Kronig relations. A nonresonant component of the refractive index of the air was computed by the following formula[7]:

$$n_0(h) = 1 + 58.2{\cdot}10^{-6}\,(1 + 7.52{\cdot}10^{-3}\,\lambda^{-2})\,P(h)/T(h),$$

0235-6880/96/05 362-06 \$02.00

where λ is the radiation wavelength, in μm; $P(h)$ is the pressure, in Torr; $T(h)$ is the temperature of the medium, in K. The account for nonresonant losses is trivial and is not considered here.

The quasiplane wave propagation was described by a system of modified Maxwell-Bloch equations (MMBE) (this modification of the standard MBE was derived in Ref. 3) which for the jth layer of the medium has the form

$$\cos\theta_j \frac{\partial E_j}{\partial h} = 2\pi i k N_j d \int_{-\infty}^{\infty} P_j(\Delta') g(\Delta_j - \Delta') \mathrm{d}\Delta', \quad \text{(1a)}$$

$$\frac{\partial P_j}{\partial \eta} = -\gamma_j P_j - i \kappa E_j, \quad \text{(1b)}$$

$$\psi_j = \psi_{j-1} + \omega t - K_j h, \quad \text{(1c)}$$

where E_j is the complex amplitude of the field, ψ_j is the fast varying optical wave phase, P_j is the complex polarization of the medium, θ_j is the wave propagation angle with respect to the normal to layers of the medium, h is the coordinate along the normal, d is the dipole moment of transition, N_j is the concentration of resonant particles, $\varkappa = 2d/\hbar$, $\gamma_j = 1/T_{2j} - i(\Delta_j - z\partial K_j/\partial\eta)$, $K_j = n_0 k/\cos\theta_j$, $k = \omega/c$, T_{2j} is the phase memory time of the medium, Δ_j is the detuning of the incident radiation from resonance, $g(\Delta)$ is the function describing inhomogeneous broadening of the resonant absorption line of the resonant component of the medium, $\eta = (t - zn_{0j}/c)$, $z = h/\cos\theta_j$, and n_{0j} is the nonresonant part of the refractive index of the medium.

The dependence of Δ_j on the spatial coordinate is caused by taking into account the center shift of the H_2O absorption line due to air pressure. The temperature dependence of the shift coefficient can be represented in the form[8]

$$\Gamma(T) = \Gamma(T_0)\ (T/T_0)^{-l},$$

where $\Gamma(T_0)$ is the shift coefficient determined under normal conditions; l is the index of temperature dependence varying from 0.7 to 1.14 for different lines of H_2O. For the average value $l \sim 0.9$, the correction to the shift coefficient along the 10-km path was about 20%. Taking into account that the errors in calculations and measurements are practically equal and that the shift due to air pressure, as a rule, exceeds that caused by temperature, the temperature dependence of the shift coefficient can be neglected in the first approximation.

The boundary condition is similar to Snell's law which is valid for optically transparent media and has the following form:

$$[n_{0,\,j-1} + n_{r,\,j-1}] \sin\theta_{j-1} = [n_{0\,j} + n_{rj}] \sin\theta_j\,. \quad \text{(1d)}$$

Here, n_{rj} is the resonant part of the refractive index of the medium; it is proportional to the imaginary part of the ratio of the induced polarization to the intensity of the optical wave field. It should be noted that one can use the propagation angle θ_{0j} calculated from the standard Snell's law without regard to n_{rj} by virtue of the fact that n_{rj} is small in comparison with n_{0j} in the left side of Eq. (1*a*). Analogously, $z = h/\cos\theta_{0j}$.

The deviations of system (1) from the standard MBE[9] are caused by consideration of the inhomogeneity of the medium.

The system (1) was solved numerically. For $T_{2j}/\tau_p < 1$ (τ_p is the pulse duration) the material equation (16) becomes singularly perturbed and the error of standard difference methods sharply increases in the transition domain $\eta/T_{2j} < 1$ (in the so-called boundary layer). In view of this fact, the approximation of Eq. (1*b*) should be performed using either nonuniform adaptive grid, what is inconvenient in the given case, or uniformly convergent algorithms. The method of exponential fitting[10] belonging to this class of algorithms was applied in our calculations. The equation (1*a*) was approximated by the trapezium rule.

The initial pulse shape was

$$E(0, t) = [\sin(\pi t/\tau_p)]^q, \quad t \in [0, \tau_p],$$
$$E(0, t) = 0, \quad t \notin [0, \tau_p]$$

and varied from quasi-Gaussian to quasi-rectangular as a function of the parameter q.

Now we present some results of calculations of the atmospheric transmission for the case of propagation of optical pulses generated by lasers along slant and vertical paths when laser generation line coincides with the water vapor absorption line.

The estimates of errors in calculating the transmission of the medium in the near-resonant domain σ due to neglect of the absorption line shift caused by air pressure are presented in Tables II–V. They are obtained as follows:

$$\sigma = [W(\Gamma) - W(\Gamma = 0)]/W(\Gamma),$$

where $W(\Gamma)$ is the transmitted pulse energy calculated for the given line shift coefficient Γ.

Range near 0.69 μm. One of the most commonly used ruby laser[6] generates in this range. Continuous frequency tuning through variation of the crystal temperature is its important advantage. The laser radiation wavelength falls within the absorption line of water vapor (λ = 694.38 nm) at the temperature T = 300 K. This line is used for sounding of the vertical H_2O profile and precisely for this line the results of calculation of energy transmission for a 10-km layer of the medium are presented in Table I as functions of the propagation direction, pulse shape and duration, and detuning from resonance. These results were obtained for the summer atmospheric model at mid-latitudes at the initial incidence angle θ = 40°.

Range near 1.064 μm. An YAG laser[11] is one of the widespread solid-state lasers operating in this range.

Three lines of water vapor absorption with intensities of 10^{-25} cm/mol fall within the laser generation band 9391–9397 cm^{-1}. They are stronger than CO_2 absorption lines in this range by an order of magnitude and stronger than O_2 absorption lines by a factor of 10^3.

Our calculations were performed for H_2O absorption lines centered at $\nu_1 = 9391.95$ cm^{-1} and $\nu_2 = 9392.50$ cm^{-1} with regard for the H_2O absorption line center shift due to air pressure that was measured experimentally at the Institute of Atmospheric Optics of the SB RAS for different propagation directions.

The results of calculating of the transmission for the summer atmospheric model at middle latitudes at the initial incidence angle $\theta = 40°$ are presented in Table II.

Range near 10.6 μm. CO_2 lasers are characterized by high efficiency, high power and energy radiated in continuous and pulsed regimes, discrete frequency tuning over a wide spectral range from 900 to 1100 cm^{-1} with a step of 1–2 cm^{-1} with the lasing lines corresponding to the vibrational-rotational transitions in the *P*– and *R*-branches of the 00^01-10^00 and 00^01-02^00 bands for a mixture of gases at pressures less than the atmospheric pressure, or by continuous tuning at pressures of 5–6 atm (Ref. 12).

Water vapor and CO_2 are main absorbing gases in the range of CO_2-laser generation; water vapor absorption is nonselective for most transitions, while the CO_2 absorption is resonant. Selective absorption by H_2O, O_3, NH_3, and other gases is observed for some transitions. In this paper, we choose just the transitions for which the absorption by H_2O is resonant, namely, 10R(22) and 9R(14) transitions of the 00^01-10^00 band and 9P(10) transition of the 00^01-02^00 band. Calculations of the shift coefficients for these transitions were performed at the Institute of Atmospheric Optics (experimental data are lacking).

The results of calculation of the absorption characteristics for the transition 10R(22) with $\lambda = 10.25$ μm are presented in Table III.

Range near 1.315 μm. The outlook for practical application of an iodine laser, generating in a narrow wavelength range near 1.315 μm, to a solution of problems of atmospheric optics depends on the fact that the radiation of this laser falls within the atmospheric transparency microwindow.[13] The atomic iodine vapor laser occupies an intermediate place between gas and solid-state lasers. As a gas laser, it has some important properties of the CO_2 laser. It is similar to the neodymium laser in radiation wavelength and way of pumping. Like in ruby and Nd^+ solid-state lasers, the working transition of the iodine lasers is a forbidden electric dipole transition, what makes it possible to produce considerable population inversion. Therefore, the iodine laser is among the most promising systems with high energy output.[6]

The main contribution to the air absorption coefficient in the spectral range near 1.315 μm comes from weak H_2O, CO_2, and CH_4 absorption lines.[14] However, the content of methane and carbon dioxide in the atmosphere is low and their contribution to the absorption in comparison with that of water vapor can be neglected.[15] Although the radiation frequency of the iodine laser ($\nu = 7603.14$ cm^{-1}) falls within the atmospheric transparency window, water vapor has an appreciable effect on the radiation.[16] It should be noted that analogous situation is observed for HF, DF, and CO_2 lasers.[16]

TABLE I. Transmission of the ruby laser pulse energy (absorbing gas is H_2O, $h = 10$ km, *middle latitudes in summer,* $\theta_0 = 40°$, *and* $\nu = 14401.34$ cm^{-1}*).*

Propagation direction	Δ, cm^{-1}			τ_p, ns	q	c, cm^{-1}/Torr
	−0.1	0	0.1			
↑	0.576	0.490	0.582	1	4	$0.223\cdot10^{-4}$
	0.549	0.391	0.561	1	1	
↓	0.535	0.475	0.535	1	4	$0.223\cdot10^{-4}$
	0.514	0.386	0.512	1	1	

TABLE II. Transmission of the neodymium laser pulse energy (absorbing gas is H_2O, $h = 10$ km, *middle latitudes in summer,* $\theta_0 = 40°$, $\nu = 9391.95$ cm^{-1}, *and* $q = 4$*).*

Propagation direction	Δ, cm^{-1}			τ_p, ns	σ, % at Δ = 0	c, cm^{-1}/Torr
	−0.1	0	0.1			
↓	0.03379	0.0337	0.03378	1		0
↓	0.04586	0.03338	0.02193	1	0.3	$0.112\cdot10^{-4}$
↑	0.0859	0.0304	0.0859	1		0
↑	0.0853	0.0306	0.0867	1	0.7	$0.112\cdot10^{-4}$

TABLE III. Transmission of the CO_2 *laser pulse energy (absorbing gas is* H_2O, h = 10 km, *middle latitudes in summer,* $\theta_0 = 40°$, $\nu = 977.43$ cm^{-1}, *and* $q = 4$).

Propagation direction	Δ, cm^{-1}: − 0.1	0	0.1	τ_p, ns	σ, % at Δ = 0	c, cm^{-1}/Torr
↑	0.0864	0.0914	0.0864	1		0
	0.0922	$1.45\cdot10^{-5}$	0.0922	10		
↑	0.169	0.0912	0.1705	1	0.2	$0.102\cdot10^{-4}$
	0.0885	$1.48\cdot10^{-5}$	0.0956	10	2.0	
↓	0.170	0.0914	0.170	1		0
	0.0906	$1.45\cdot10^{-5}$	0.0906	10		
↓	0.0972	0.0834	0.0739	1	9.6	$0.102\cdot10^{-4}$
	0.0872	$1.47\cdot10^{-5}$	0.094	10	1.3	

TABLE IV. Transmission of the iodine laser pulse energy (absorbing gas is H_2O, h = 10 km, *middle latitudes in summer,* $\theta_0 = 40°$, $\nu = 7602.35$ cm^{-1}, *and* $q = 4$).

Propagation direction	Δ, cm^{-1}: − 0.1	0	0.1	τ_p, ns	σ, % at Δ = 0	c, cm^{-1}/Torr
↑	0.327	0.217	0.328	1	0	$0.525\cdot10^{-5}$
	0.272	$5.14\cdot10^{-3}$	0.287	10	0	
↓	0.225	0.204	0.217	1	6	$0.525\cdot10^{-5}$
	0.271	$5.14\cdot10^{-3}$	0.277	10	0	
↑	0.327	0.217	0.327	1		0
	0.275	$5.14\cdot10^{-3}$	0.275	10		
↓	0.227	0.217	0.222	1		0
	0.274	$5.14\cdot10^{-3}$	0.274	10		

TABLE V. Transmission of the iodine laser pulse energy (absorbing gas is H_2O, h = 10 km, *middle latitudes in summer,* $\theta_0 = 40°$, $\nu = 7600.79$ cm^{-1}, *and* $q = 4$).

Propagation direction	Δ, cm^{-1}: − 0.1	0	0.1	τ_p, ns	σ, % at Δ = 0	c, cm^{-1}/Torr
↑	0.0923	0.0385	0.0927	1	0	$0.278\cdot10^{-5}$
	0.0229	$5.17\cdot10^{-8}$	0.0237	10	0.2	
↑	0.0906	0.0317	0.0944	1	22	$0.267\cdot10^{-4}$
	0.0194	$6.34\cdot10^{-8}$	0.0271	10	18	
↑	0.0925	0.0385	0.0925	1		0
	0.0233	$5.18\cdot10^{-8}$	0.0233	10		
↓	0.0389	0.0383	0.0340	1	1	$0.278\cdot10^{-5}$
	0.022	$5.41\cdot10^{-8}$	0.0230	10	0.4	
↓	0.0560	0.0227	0.0175	1	70	$0.267\cdot10^{-4}$
	0.0189	$6.04\cdot10^{-8}$	0.0263	10	11	
↓	0.0364	0.0387	0.0364	1		0
	0.0226	$5.39\cdot10^{-8}$	0.0226	10		

An approximate relative contribution, in per cent, from wings of some H_2O lines into the absorption at a frequency of 7603.14 cm^{-1} was given in Ref. 16. Absorption at 7603.14 cm^{-1} is caused by only five H_2O lines and about 55% of it is due to the line with $\nu = 7602.35\ \text{cm}^{-1}$. So in the present paper the calculations were performed for the H_2O absorption line with $\nu = 7602.35\ \text{cm}^{-1}$ in addition to the water vapor absorption line with $\nu = 7600.79\ \text{cm}^{-1}$ for which the peculiarities of short optical pulse propagation along slant paths in the resonantly absorbing atmosphere have been already analyzed.[2,5] The results of calculations are presented in Tables IV and V.

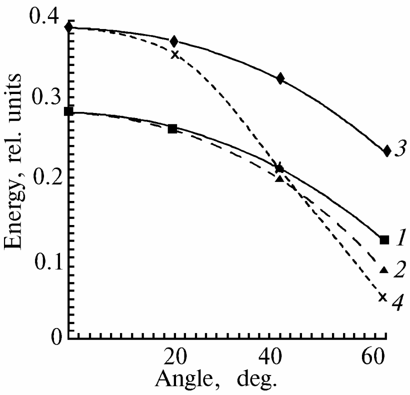

FIG. 1. Energy of the iodine laser radiation ($\nu = 7602.35\ \text{cm}^{-1}$) *transmitted along slant atmospheric paths: 1,3) upward propagation direction; 2,4) downward propagation direction; 1,2) zero frequency detuning; 3,4) detuning* $\Delta = 0.1\ \text{cm}^{-1}$. *Pulse duration is* 1 ns.

Figure 1 shows variations of pulse energy of the iodine laser radiation as functions of the tilt angle and propagation direction for the pulse duration $\tau_p = 1$ ns. Curves *1* and *2* are for zero detuning from resonance, and curves *3* and *4* are for the detuning $\Delta = 0.1\ \text{cm}^{-1}$. The solid lines are for the upward direction of the optical pulse propagation along slant paths and the dashed lines are for the downward direction of propagation. For pulse duration $\tau_p = 10$ ns, the propagation direction affects insignificantly the transmitted energy, whereas the tilt angle is the decisive factor. When the propagation direction is changed by 20°, the transmitted energy decreases by a factor of 10^2 (at zero detuning).

Let us formulate briefly the main conclusions of this paper, connected with the attenuation of pulse radiation of ruby, neodymium, iodine, and CO_2 lasers by H_2O vapor in the atmosphere estimated here.

It has been demonstrated[3] that for the reverse direction of pulse propagation along slant atmospheric paths under conditions of resonant absorption, transmitted pulse energy may change. This phenomenon is caused by the variations of the beam refraction angle accompanying the temporal variations of the resonant part of the refractive index of the medium due to nonstationarity of the interaction. The effect has been also estimated in Ref. 3 for some generation lines of the above-mentioned lasers.

Since the temperature, density, and pressure of the real atmosphere have random spatial distribution due to turbulent air motion, it is necessary to estimate the influence of this factor on the above-indicated mechanism of nonstationary distortion of optical pulses. As shown in Ref. 3, the radiation of different parts of a short optical pulse (leading edge, central part, and trailing edge) will propagate along different trajectories under these conditions. It is obvious that the influence of the turbulence should be taken into account if the trajectories pass through different random inhomogeneities of the medium because the phase difference of different parts of the pulse will change stochastically at the exit from the medium.

Let us estimate the angle of spatial beam divergence due to temporal fluctuations of the resonant part of the refractive index of the medium. For the surface atmosphere, the typical value of the resonant part of the refractive index n_r is approximately equal to 10^{-10}. Temporal variations of the refraction angle at the interfaces between the layers of the medium $\delta\theta_j(t)$ can be estimated by Eq. ($1d$) as follows:

$$\delta\theta_j(t) \sim \frac{n_{0,j-1}}{n_{0j}} \left(\frac{n_{r,j-1}}{n_{0,j-1}} - \frac{n_{rj}}{n_{0j}} \right).$$

Assuming $n_{0j} = 1$, the order of magnitude

$$\delta\theta_j \sim \max\,(n_{r,j-1} - n_{rj}) \le 10^{-10}.$$

Spatial divergence of the beam $\Delta\rho$ can be estimated from the formula $\Delta\rho \sim \delta\theta z$, where z is the path length. In our calculations, z ˜ 10 km and hence $\Delta\rho \le 10^{-4}$ cm. Since $\Delta\rho$ is considerably less than the internal turbulence scale (˜mm, see Ref. 7), the phase difference for different parts of the pulse for a given beam will be regular, and the turbulence will not affect the process of nonstationary distortion of the optical pulse in the atmosphere.

The second result of the paper is connected with estimates of the influence of the absorption line center shift due to air pressure on the atmospheric transmission. The essential feature of our calculations is that we took into account nonmonochromaticity of the radiation due to its pulse character. The results of calculations demonstrate that neglect of the line shift may result in the errors in estimating the transmission of the medium exceeding (sometimes considerably) the typical values of the experimental error and analogous estimates obtained for narrow-band radiation.[8] The latter fact requires some comments because, at first sight, the decrease of pulse duration leads to widening of its spectrum what, in its turn, must diminish the influence of the value of detuning from resonance on the transmission of the medium.

This result is explained by the fact that nonstationary refraction caused by the resonant component of the medium changes the integrated absorption characteristics of the medium including the transmission (see Ref. 3 and Tables I–V of the present paper). Besides, nonstationary refraction is absent at resonance and is maximum for detuning by half-width of the absorption line.

Thus, the influence of the absorption line shift due to air pressure in the spectral range close to resonance in the process of propagation of pulse radiation cannot be reduced only to the change of the absorption coefficient of the medium, as it takes place for the narrow-band radiation. In addition, the line shift results in the change of the transmission of the medium due to nonstationary refraction.

ACKNOWLEDGMENTS

The authors express their gratitude to N.N. Lavrent'eva and Yu.A. Poplavskii for kindly given data on the shift coefficients of H_2O lines and to A.D. Bykov and K.M. Firsov for useful discussion.

REFERENCES

1. V.E. Zuev, *Propagation of Laser Radiation in the Atmosphere* (Radio i Svyaz', Moscow, 1981), 288 pp.
2. M.V. Kabanov, Yu.V. Kistenev, and Yu.N. Ponomarev, Atm. Opt. **2**, No. 2, 135–139 (1989).
3. M.V. Kabanov, Yu.V. Kistenev, and Yu.N. Ponomarev, Atm. Opt. **4**, No. 3, 205–207 (1991).
4. V.V. Zuev, et al., Opt. Lett. **10**, No. 7, 318–320 (1985).
5. M.V. Kabanov, Yu.V. Kistenev, and Yu.N. Ponomarev, Atm. Opt. **2**, No. 3, 260–262 (1989).
6. A.A. Mitsel' and Yu.N. Ponomarev, *Optical Models of the Molecular Atmosphere* (Nauka, Novosibirsk, 1988), 128 pp.
7. J.W. Strohbehn, ed., *Laser Beam Propagation in the Atmosphere* (Springer-Verlag, Berlin–Heidelberg–New York, 1978).
8. A.D. Bykov, Yu.N. Ponomarev, and K.M. Firsov, Atmos. Oceanic Opt. **5**, No. 9, 595–605 (1992).
9. L. Allen and J.H. Eberly, *Optical Resonance and Two-Level Atoms* (Willey, New York, 1976).
10. E.P. Doolan, J.J.H. Miller, and W.H.A. Schilders, *Uniform Numerical Methods for Problems with Initial and Boundary Layers* (Dublin, 1980).
11. A.A. Mitsel', V.P. Rudenko, L.N. Sinitsa, and A.M. Solodov, Opt. Atm. **1**, No. 5, 43–47 (1988).
12. N.V. Karlov, *Lectures on Quantum Electronics* (Nauka, Moscow, 1983), 319 pp.
13. B.G. Ageev, A.Yu. Kurov, V.D. Nikolaev, et al., Izv. Vyssh. Uchebn. Zaved. Ser. Fiz. **29**, No. 6, 96–98 (1986).
14. L.S. Rothman, Appl. Opt. **20**, No. 5, 791–795 (1981).
15. V.A. Filimonova and K.M. Firsov, Izv. Vyssh. Uchebn. Zaved. Ser. Fiz., Deposited in VINITI, No. 2681–B94 (1994), 20 pp.
16. S.L. Bragg and J.D. Kelley, Appl. Opt. **26**, No. 3, 506–513 (1987).